

This article was downloaded by:

On: 28 January 2011

Access details: *Access Details: Free Access*

Publisher *Taylor & Francis*

Informa Ltd Registered in England and Wales Registered Number: 1072954 Registered office: Mortimer House, 37-41 Mortimer Street, London W1T 3JH, UK



## Physics and Chemistry of Liquids

Publication details, including instructions for authors and subscription information:

<http://www.informaworld.com/smpp/title~content=t713646857>

### Molecular Dynamics of Binary Fluids in the Region of the Critical Mixing Point: I. Experimental Fundamentals and the Adjustment of the Lennard-Jones Potential Parameters

Claus Hoheisel<sup>a</sup>

<sup>a</sup> Lhrstuhl für Theoretische Chemie, Ruhr-Universität Bochum, Bochum, Federal Republic of Germany

**To cite this Article** Hoheisel, Claus(1980) 'Molecular Dynamics of Binary Fluids in the Region of the Critical Mixing Point: I. Experimental Fundamentals and the Adjustment of the Lennard-Jones Potential Parameters', *Physics and Chemistry of Liquids*, 9: 3, 245 – 264

**To link to this Article:** DOI: 10.1080/00319108008084780

**URL:** <http://dx.doi.org/10.1080/00319108008084780>

PLEASE SCROLL DOWN FOR ARTICLE

Full terms and conditions of use: <http://www.informaworld.com/terms-and-conditions-of-access.pdf>

This article may be used for research, teaching and private study purposes. Any substantial or systematic reproduction, re-distribution, re-selling, loan or sub-licensing, systematic supply or distribution in any form to anyone is expressly forbidden.

The publisher does not give any warranty express or implied or make any representation that the contents will be complete or accurate or up to date. The accuracy of any instructions, formulae and drug doses should be independently verified with primary sources. The publisher shall not be liable for any loss, actions, claims, proceedings, demand or costs or damages whatsoever or howsoever caused arising directly or indirectly in connection with or arising out of the use of this material.

# Molecular Dynamics of Binary Fluids in the Region of the Critical Mixing Point

## I. Experimental Fundamentals and the Adjustment of the Lennard–Jones Potential Parameters

CLAUS HOHEISEL

*Lehrstuhl für Theoretische Chemie, Ruhr-Universität Bochum,  
D 4603 Bochum, Federal Republic of Germany*

*(Received November 12, 1979)*

In two subsequent articles we shall report our molecular dynamics investigations for the three partially miscible fluid mixtures  $\text{CH}_4/\text{CF}_4$ ;  $\text{Ne/Kr}$ ;  $\text{He/Xe}$ . The goal of these studies was the simulation of these mixtures at the larger vicinity of the critical mixing point and the investigation of the microscopic behaviour.

This first part describes basic aspects of modelling a critical point by molecular dynamics calculations (MDC) and examines the experimental and theoretical data for the larger neighbourhood of a critical mixing point of binary fluids.

For the systems under study it is shown that Lennard–Jones type potentials can serve as an appropriate basis for MDC. The adjustment of the Lennard–Jones potential parameters of the 1–2 interaction was done in terms of the parameters occurring in the Redlich–Kwong equation of state.

The second article<sup>1</sup> is concerned with the actual MD-results on the static and dynamic microscopic structure of the mixtures for the region of the critical mixing point. It is shown that the near-critical range of the systems is simulated reasonably by our MDC.

## 1 INTRODUCTION

The study of critical points of various many-body systems has always been a difficult task for experimentalists and theorists. However, the understanding of the behaviour of systems near a critical point has greatly been improved in the period of the last 20 years. This has been primarily achieved by improved experimental techniques of scattering measurements by light, x-ray and neutrons. Furthermore there were modern theoretical treatments

available, as the renormalisation group and the mode-mode coupling, which allowed a deeper view into the nature of critical phenomena.

Though for pure substances and multiple-component systems the vicinity very close to a critical point,  $|T - T_c| \lesssim 1$  K ( $T_c$  critical temperature), is well investigated experimentally and theoretically, there was much less attention paid to the larger region around a critical state. This is clear from the following facts: most of the measurable properties of fluids and magnetizable systems change anomalously only very near the critical state. Furthermore for the current theories it is often assumed that the correlation length of the systems is large compared with a few interparticle-distances.

Consequently reasonable comparisons of the theory and experiment are actually possible for states very close to the critical point, where the correlation length of most of the systems has sharply increased. The modern scattering experiments by x-ray and neutrons are principally able to give information about the microscopic behaviour of systems in this interval between a non-critical state and a state very near the critical one. Unfortunately such experiments are very complicated, particularly, when x-ray as well as neutrons are to be used for a row of thermodynamic states.<sup>2</sup>

So far only a few experiments have been performed to investigate the *near-critical* region. The term *near-critical* region is introduced here as a short definition of the above described broader interval around the critical point,  $1 \text{ K} \lesssim |T - T_c| \lesssim 10 \text{ K}$ . The results of these studies yielded only quantitative conclusions and have hardly increased our knowledge about the static and dynamic microscopic processes in this region of a critical point.<sup>3</sup> It was commonly accepted that the nearest neighbourhood of the molecules remains nearly unchanged, when the critical point is approached.

A further lack of information about critical phenomena has arisen from the fact that currently there are no theoretical treatments of a fluid at a critical point. All existent theories are based on lattice-gas models. Although from the universality principle it is concluded that lattice and fluid systems exhibit the same critical behaviour, it has not explicitly been shown that non-localized particles behave like localized ones, when the correlation length of the particle systems is appreciably larger than the interparticle-distance.<sup>4</sup>

Computer-simulation-methods have frequently been used to study many-body systems in condensed phase, and the results of these calculations have much improved our understanding of liquids and fluids. For non-critical systems a lot of molecular dynamics calculations and Monte-Carlo calculations have been carried out to determine the microscopic properties, which at time are not accessible by experiment.

In general these model calculations are performed with ensembles of 100-1000 particles, where the size of the systems is not greater than about

$1.25 \times 10^5 \text{ \AA}^3$ . Systems of such finite size will however not exhibit a critical point, consequently a critical state cannot directly be described by computer calculations.

Nevertheless it should be possible to simulate approximately the near-critical region of experimental systems or models by machine calculations, as long as the correlation length of the near-critical system is comparable to the microscopic length of the "computer-ensemble."

Therefore the study of a near-critical region using computer simulation methods is on one hand very limited, but on the other hand the results of the calculations can reasonably be checked and if necessary improved by varying the number of particles and periodic boundary conditions.

This has been illustrated through Monte-Carlo calculations on magnetizable systems near the Curie-point. In a few instances, Binder<sup>5</sup> has even evaluated critical exponents from his calculations, which agree well with those experimentally found or theoretically predicted. The modelling of a near-critical state of a simple lattice spin-system is not so complicated as that of a fluid, but the problem of the finiteness of the systems at a critical point occurs in both cases.

To our knowledge there are no computer-simulation-calculations, neither for pure fluids nor for fluid mixtures, which in detail treat the microscopic properties of systems near the critical region.<sup>5,6</sup> However, Adams<sup>7</sup> has recently shown that Monte-Carlo calculations are able to reproduce reasonably the region near a critical point of a "Lennard-Jones-fluid." By using the experimentally known critical exponents he extracted realistic critical values for the temperature, the pressure and the density. These results indicate that fluid systems can be realistically simulated in the range of a critical point.

Our molecular dynamics calculations on mixtures have primarily been performed to elucidate the following questions:

- a) Is it possible to simulate the main features of the near-critical region of a simple binary fluid mixture on the basis of effective pair-potentials.
- b) What information is available about the molecular processes leading to a critical state.

Binary mixtures are generally less suited for simulation-calculations than pure fluids due to the three potential functions describing the three interactions. This drawback, however, seemed to be acceptable in view of several advantages. For the critical region, the density of a mixture is much less temperature dependent and therefore experimentally known much more accurately than the density of a pure substance.<sup>8,9</sup> Binary liquid mixtures exhibit critical phenomena in a larger interval around the critical point than

one-component systems do.<sup>10</sup> Pertaining to MDC, a binary system apparently is more stable against local concentration fluctuations than a monomolecular system against density fluctuations.<sup>11,12</sup>

Our calculations were carried out to simulate the experimental systems: CH<sub>4</sub>/CF<sub>4</sub>; Ne/Kr and for further comparisons He/Xe. Significant results were obtained in terms of the static and dynamic pair-distribution functions and by the self-diffusion coefficients of these mixtures.

## 2 THE CRITICAL POINT AND THE NEAR-CRITICAL REGION

In a binary liquid mixture we have instead of a critical point of a pure liquid a critical line, along which at least two of the coexistent phases become identical with respect to their intensive variables<sup>13,14</sup>. The phases can be part of the thermodynamic gas-liquid range (L-G) or only of the pure liquid range (L-L). The latter case is called a critical phase separation. The phase-diagrams of partially miscible multiple-component systems often exhibit a very complex shape and can be interpreted for only a few groups of substances.<sup>4,15</sup> For example, if the critical mixing temperatures of those systems lie above the critical temperatures of the pure components, as it is found for a few rare-gas mixtures under high pressure, this is named a "gas-gas phase separation." For multiple-component systems it is furthermore possible to observe a so-called tricritical point, at which three phases become identical.<sup>10,15</sup>

The thermodynamic conditions for a binary fluid mixture showing a critical mixing point can be formulated in analogy to those for a pure substance. As function of concentration  $x$  the chemical potential  $\mu$  of a mixture has a point of inflection with a horizontal tangent at the critical mixing point and at constant  $T$  and  $P$ :

$$\left(\frac{\partial\mu}{\partial x}\right)_{T,P} = 0 \quad \left(\frac{\partial^2\mu}{\partial x^2}\right)_{T,P} = 0 \quad (1)$$

The higher derivatives of  $\mu$  are also allowed to vanish, but it can be proved that the first non-vanishing one has to be odd and positive.<sup>10,14</sup>

From the relations (1) it is clear that in general the two-component systems have critical lines due to the Gibbs' phase rule, because (1) holds for different values of  $T$  and  $P$ .

Since the inverse osmotic compressibility is proportional to  $\partial\mu/\partial x$ , we derive from (1) that the osmotic compressibility diverges at the critical mixing point. Consequently in a binary mixture, large local concentration fluctuations should occur at the critical point, because differences between local compositions cannot be rebalanced. This has experimentally been

proven for a number of binary systems in terms of the binary diffusion coefficient  $D_{12}$ . From theoretical arguments it is derivable that  $D_{12}$  varies proportionally to the concentration gradient of the chemical potential  $\partial\mu/\partial x$ .<sup>16,17</sup> In so measuring the binary diffusion coefficient  $D_{12}$  we are able to determine  $\partial\mu/\partial x$ . The vanishing of  $D_{12}$  at the critical mixing point is confirmed several times.<sup>17,18</sup> For the mixture Water/Triethylamine a decrease of  $D_{12}$  has been observed of about two orders of magnitude, when the critical temperature,  $T_c$ , was approximated in the range of  $T_c + 1$  to  $T_c + 0.1$  K.<sup>18</sup>

A row of further quantities behaves anomalously† at the critical mixing point, as is known from experimental experience. The specific heat and the stress-viscosity increase sharply in this region.<sup>19–21</sup> The sound-velocity falls down close to the critical point.<sup>22</sup> The surface tension seems to behave anomalously, although for binary mixtures this property is less investigated.<sup>4</sup>

In contrast to this the thermal conductivity and the self-diffusion exhibit the usual behaviour near the critical mixing point.<sup>3,23</sup> For instance the self-diffusion coefficient of a few binary liquids showed no anomalies, even 0.05 K close to the critical temperature.<sup>23</sup>

The molecular processes and the structure of critical mixtures are directly investigated by scattering experiments with rays of various wave-length. Visible light of a wave-length of  $\sim 5000$  Å give important knowledge about the long-range order in fluids at the close vicinity of the critical point.

X-ray and neutrons complementarily provide information about the near and nearest neighbourhood of molecules in non-critical and near-critical systems.<sup>24</sup>

The quantitative, light-optical indication of critical phenomena is obtainable in the range of 1–2 K near the critical point of a mixture.<sup>25</sup> For instance, Fürth and co-workers<sup>26</sup> have determined integral pair-correlation functions from light scattering measurements on a number of binary systems. Their experiments indicated an increase of the coherence length of about 50%, when the temperature varied from  $T_c + 0.3$  to  $T_c + 0.05$  K at the critical concentration. Then the absolute range of the coherence length already amounts to 1000–3000 Å.

Far away and at a moderate distance from the critical mixing point, light-scattering can only provide qualitative information. For example: The system  $\text{CH}_3\text{-OH}/\text{CS}_2$  begins to show critical opalescence already 8–10 K above the upper critical solution point, whereas for the mixture  $\text{C}_7\text{F}_{14}/\text{C}_7\text{H}_{16}$  a weak opalescence is visible 3–5 K above the critical temperature.<sup>27</sup> Similar observations have been made in scattering measurements by acoustic

† 'Anomalous' is used in the sense that at the critical point a quantity exhibits a differing behaviour as function of a chosen variable compared to that at non-critical conditions.

waves, despite the fact that mechanic waves have a wave-length of a factor  $10^3$ – $10^4$  greater than light. Chynoweth and Schneider<sup>28</sup> have discovered an appreciably anomalous absorption of sound already 8 K below the lower critical mixing point of the mixture Water/Triethylamine.<sup>29</sup>

X-ray scattering experiments, in contrast, provide detailed quantitative knowledge of a system in the near-critical region, particularly, of molecular spheres of 10–100 Å. Brady and co-workers<sup>30</sup> have performed small-angle x-ray scattering measurements on the system  $C_7F_{16}/i-C_8H_{18}$ . Their experiments resulted in an estimation of the average cluster-volume occupied by the molecules of the same kind at about 4 K above the critical temperature of the system. From that cluster-volume of a symmetric cylinder of  $5.4 \times 10^4$  Å<sup>3</sup>, we roughly obtain a correlation length of about 45 Å. This value is in agreement with the numbers evaluated from modern measurements on the system Cyclohexane/Aniline.<sup>31</sup>

The authors of these later experiments derived a coherence length of about 30 Å for  $T - T_c \sim 4$  K. We will refer back to the latter measurements in the following paragraph.

Even for the remarkable distance of about 15 K away from the critical point, Brady and co-workers<sup>32</sup> were able to prove a significantly increased coherence length of the system  $C_7F_{16}/i-C_8H_{18}$ .

The radius of gyration therein determined by an analysis of the scattering data, can roughly be converted to the coherence length, and a value of about 20 Å is retained for  $T - T_c \approx 16.5$  K. This value, too, falls in line with the measurements on the system Cyclohexane/Aniline, which yielded  $\sim 15$  Å for  $T - T_c \sim 15$  K.<sup>31</sup>

Unfortunately most of the further small-angle x-ray scattering experiments have been done very close to the critical solution temperature, so a more extensive comparison with other studies is not possible.

Nevertheless, the results reported above are gathered from independent work and they indicate that very differing binary fluid mixtures behave similarly in the near-critical region. In view of that it appears justified to compare directly our present simulation-calculation-results with these experimental data of other systems.

### 3 CORRELATION FUNCTIONS, CORRELATION LENGTH

Our modern understanding of the structure and dynamic processes of molecular many-body systems is primarily obtained by means of the static and dynamic correlation functions. Especially fluid systems can be characterized in terms of these correlation functions, since microscopic models for fluids are generally not to be based on a lattice structure. Two of the most important

correlation functions are the radial pair-distribution functions  $g(r)$  and the dynamic pair-distribution function  $G(\mathbf{r}, t)$ . Van Hove<sup>33</sup> was the first who has discussed the connection between  $G(\mathbf{r}, t)$  and scattering data of neutrons on magnetizeable systems. He split this function into two parts:

$$G(\mathbf{r}, t) = G_s(\mathbf{r}, t) + G_d(\mathbf{r}, t) \quad (2)$$

Where the  $G_s$  is called the self-term and  $G_d$  the distinct-term.  $G_s$  governs the self-diffusion process of the system, while  $G_d$  characterizes the collective behaviour of the particles. The function  $G_d(\mathbf{r}, t = 0)$  is identical with  $g(r)$ , if  $G_d$  is appropriately normalized. Both functions  $G_s$  and  $G_d$  are accessible from neutron-scattering experiments and computer-simulation studies.

In experiments frequently the Fourier transforms of these correlation functions are determined. These so-called structure factors  $S(\mathbf{k})$  and  $S(\mathbf{k}, \omega)$  depend on the intensity and the spectrum of the scattering waves. In particular, the static structure factor  $S(\mathbf{k})$  ( $\mathbf{k}$  wave-vector) is proportional to the total cross section assuming the static approximation.<sup>34</sup> The dynamic structure factor  $S(\mathbf{k}, \omega)$  ( $\omega$  angle-frequency) is measured through the twofold differential cross-section.<sup>35</sup>

Near a critical point it is necessary to attain high resolution to determine significantly  $S(\mathbf{k}, \omega)$ . The modern laser light spectrometers, however, allow the evaluation of  $S(\mathbf{k}, \omega)$  even at  $|T - T_c| \approx 10^{-3} \text{ K}$ .<sup>35</sup>

Clearly the complete determination of these correlation functions is not achievable, since the range of  $(\mathbf{k}, \omega)$  investigated by experiments or simulations is often very limited. In many cases it is not even possible to obtain a reasonable Fourier inversion of the actual data.<sup>36</sup>

The entire information about the correlation functions is desirable for a  $(\mathbf{k}, \omega)$ -range, which covers the complete coherence range of the system.

For a system extremely close to a critical point we consequently have to know the correlation functions over an immense  $(\mathbf{k}, \omega)$ -range due to the increased correlation length of the system. It turned out, however, that in critical systems the spectrum of long wave-lengths and low frequencies is governing the properties of the system, so that the evaluation of the correlation functions for this  $(\mathbf{k}, \omega)$ -region is sufficient.<sup>37,38</sup>

In contrast to this, our investigation of the near-critical region requires the knowledge of the correlation functions over the whole coherence range of the system, if specifically the transition from a non-critical state to a critical state is to be studied. Our MDC have therefore been extended as far as possible to derive the correlation functions for a wide  $(\mathbf{r}, t)$ -range.

A critical or a near-critical system is microscopically defined by an increased coherence length. This molecular parameter of length essentially describes the range of order in a system and is therefore closely related to the



net pair-distribution function  $h(r) = g(r) - 1$ . An exact definition is frequently introduced by the second moment of  $h(r)$ :<sup>10</sup>

$$\xi^2 = \frac{1}{6} \int r^2 \cdot h(r) \cdot dr \Big/ \int h(r) \cdot dr \quad (3)$$

or by means of the asymptotic behaviour of  $h(r)$  for large  $r$ . After Ornstein–Zernike<sup>39</sup> the net pair-distribution function  $h(r)$  exhibits an exponential decrease for large  $r$ :

$$h(r) = f(r) \cdot \exp\left(-\frac{r}{\xi}\right) \quad (r \rightarrow \infty) \quad (4)$$

Where  $f(r)$  designates a weakly  $r$ -dependent function and  $\xi$  is the logarithmic decrement of the envelope of  $h(r)$ .<sup>31,37</sup>

Sufficiently away from the critical state  $h(r)$  disappears within a few intermolecular distances, so that  $\xi$  commonly amounts to 5–10 Å. At the critical point, however, the coherence length diverges and the integrals in (3) become infinite. The exponential part in (4) has to be dropped, and  $h(r)$  is long-range. Near the critical point,  $|T - T_c| \lesssim 1$  K, the definitions of (3) and (4) can be used in a modified form, if scaling-relations for  $\xi$  are included.<sup>40</sup> At this close vicinity of the critical point there are mainly three methods to determine  $\xi$  for a binary fluid mixture by light-scattering experiments:<sup>31,41</sup>

- a) Measuring the differential cross-section, i.e. evaluating the local distribution of the intensity of the scattered light.
- b) Measuring of the total cross-section, i.e. determination of the turbidity.
- c) Determination of the half-width of the Rayleigh line from the spectrum of the scattered light.

In contrast to these investigations very near the critical point, we have studied the near-critical region of several mixtures by means of simulation calculations. Direct experimental knowledge about the near-critical region can only be obtained by x-ray and neutrons, as we have already explained in Section 2. There is however one possibility to assess the correlation length in the near-critical region of binary systems by light-scattering experiments. Volochine and co-workers<sup>31</sup> have combined experimental results with theoretically derived relations and they were able to prove a significant dependence of  $\xi$  from temperature, up to the appreciably large distance of  $T - T_c \sim 30$  K. Volochine applied the Einstein–Stokes–Kawasaki formula on the binary diffusion coefficient  $D_{12}$ :

$$D_{12} = \frac{k_B \cdot T}{6\pi\eta \cdot \xi} \quad (5)$$

and measured the  $D_{12}$  of the system of Cyclohexane/Aniline as function of temperature in terms of the half-width of the Rayleigh line.<sup>35</sup> The viscosity

values  $\eta$  thereby were taken from Arcovito's work.<sup>42</sup> By this method he obtained a linear correlation between the coherence length  $\xi$  and the temperature difference,  $T - T_c$ , in a twofold logarithmic plot, as expected from the scaling law for  $\xi$ . However, the range the plot was valid for turned out to be surprisingly large. For a temperature range of  $1 \text{ K} \lesssim T - T_c \lesssim 30 \text{ K}$ ,  $\xi$  varied between  $8 \text{ \AA} \lesssim \xi \lesssim 90 \text{ \AA}$ . Beyond  $T - T_c > 30 \text{ K}$  there was no further alteration of  $\xi$ , the coherence length remained at the value of  $\sim 8 \text{ \AA}$ . These findings agree with the x-ray scattering investigations of Brady already reported in Section 2, and show definitely that for partially miscible liquid mixtures of critical composition, the (homogeneous) system behaves non-critically only in a temperature region considerable distant from the critical solution temperature.<sup>43</sup>

The results of our simulation calculations indicate similar phenomena for the binary fluid mixtures studied herein. It can be concluded from our calculations that the mixtures considered for simulation show near-critical behaviour up to  $T - T_c^p \sim 25 \text{ K}$ , where  $T_c^p$  is the estimated pseudo-critical temperature of the model system (see next paragraph).

Analogous to the coherence length  $\xi$  one has to consider the characteristic time constant  $t_c$ , i.e. a characteristic frequency  $\omega_c = 1/t_c$  of a system.  $t_c$  is the microscopic time parameter of the system and can be defined similarly in the Eqs. (3) and (4) by the time-dependent pair-distribution function  $G(\mathbf{r}, t)$ .

Under critical conditions  $t_c$  diverges together with the correlation length  $\xi$ . This is experimentally verified and is known as the "critical slowing down."<sup>35,43</sup> The increase of  $t_c$ , i.e. the decrease of  $\omega_c$ , near a critical point, is accessible from Brillouin scattering experiments, which give the dynamic structure factors  $S(\mathbf{k}, \omega)$  for the interesting region, as mentioned before.<sup>35,45</sup>

For our simulations, we have determined  $t_c$  directly from the time-dependent envelope of  $G_a(r, t)$ .

#### 4 FINITE SYSTEM

For every many-body system that involves a finite number of particles  $N$ , the statistical mechanical partition function  $Z(\Phi, \Lambda, N)$  is built up by a finite sum of analytic terms of the corresponding thermodynamic variables defined for an arbitrary, physically reasonable range. A thermodynamic quantity constructed from the derivatives of  $\ln Z$  has consequently to be analytical, too, and cannot exhibit any singularities. A critical phase-transition characterized by such a singular behaviour of thermodynamic properties is therefore not possible for finite systems.<sup>46</sup>

In particular, a model system will not exhibit a critical point, if its size is limited in the sense that the correlation length is restricted at the critical

point. In this rigorous sense no experimental system is able to show a critical state. However, for practical purposes it is sufficient to study systems whose size is large enough to show coherence lengths of orders of magnitude greater than the average-distance of the particles involved. That condition is certainly accomplished for all macroscopic liquid systems.

For simulation calculations on finite systems we have to pay great attention to the fact that the model system approaching the critical point of the ideal infinite system will be increasingly less able to describe critical conditions of the ideal system. These effects due to the finite shape of the model system are known as "rounding-effects." By rounding we mean the distorted behaviour of properties of a finite system near its "phase-transition" compared to that of the pertaining infinite system. For instance, the specific heat capacity of a mono-system diverges at the critical point; the corresponding finite system does exhibit a similar rising of the heat capacity by approaching the critical temperature (of the ideal system), but in this case the values go through a maximum and the position of the maximum is shifted with respect to temperature. In other words, the finite system has its own pseudo-critical point, where "weaker" critical phenomena are found than in the ideal system.<sup>5,40</sup> For Ising-models it can be shown that the limitation of only one dimension of the system effects drastically the critical exponents.<sup>5,46</sup> Details are found in Ref. 5.

Considering computer-simulation calculations we expect erroneous computation results, when the coherence length  $\xi$  has reached the significant length of the ensemble volume, often half the length of a cubic box.<sup>†</sup>

The magnitude of these deviations near a critical point can be estimated by calculations with ensembles of different particle numbers. Pertaining to this, Monte-Carlo computations on spin-systems with  $N = 54$  up to  $N = 1728$  particles have generated valuable information.<sup>5</sup> For fluids this kind of simulation has hitherto not been performed, since in this case one has to treat three-dimensional systems and the change of the particle number has little effect on the size of the model-box.

## 5 MOLECULAR DYNAMICS CALCULATIONS ON SIMPLE PARTIALLY MISCIBLE BINARY SYSTEMS

### 5.1 Method

The method of MDC is now well established and should not be described in the following text.<sup>47,48</sup> We will, however, give an outline of the technical details involved in our calculations on the three systems studied herein. The

---

<sup>†</sup> The usual definition of  $\xi$  refers to the *diameter* of the ordered range of particles i.e. of the volume of the 'particle-cluster,' whereas here it always refers to the *radius*.

TABLE I  
Technical details of the MD-runs

System	$N$	$\Delta t$ [s]	$r_c$ [ $\sigma_1$ units]	$n_N$	$n_E$
I CH <sub>4</sub> /CF <sub>4</sub>	256	$1 \cdot 10^{-14}$	2.8–3.0	500–2000	2000–4000
II Ne/Kr	256–864	$1 \cdot 10^{-14}$	2.8–3.3	500–1000	2000–5000
III He/Xe	864	$5 \cdot 10^{-15}$	3.2	1000	3000

$\Delta t$  integration step.

$N$  number of particles.

$r_c$  cut-off radius.

$n_N$  equilibration steps.

$n_E$  steps after equilibration.

length of the runs and the size of the ensembles are presented in Table I. For most instances the maximum values given in this table refer to near-critical conditions of the systems.

Temperature and pressure without long-range corrections were evaluated during the equilibrium-runs. The temperatures fluctuated less than 0.2 K. The accuracy of the pressure values corrected for the potential cut-off distance is estimated to be about 10% for system II and 15% for system III. For system I we avoided an estimation of error-bars on the grounds mentioned later. For all the temperatures, the pressure of system II and system III was constant at  $1940 \pm 30$  bar and  $790 \pm 30$  bar, respectively.

The evaluation of the time-independent and time-dependent pair-distribution functions (PDF) was carried out by averaging 100–300 configurations for system I and 700–3000 for the systems II and III per run. We performed 5–6 runs per thermodynamic state for system I, and 3–5 runs per state for the systems II and III. For the PDF the average-error is estimated to be 2% pertaining to the systems II and III and 8% to system I. The self-diffusion coefficients (SDC) have been determined by the mean-square displacements of particles for system I. For the systems II and III, the SDC were calculated both from the mean-square displacements and from the velocity auto-correlation function (VACF).<sup>49</sup>

The error-bars amount to 10% for system I and to 5% for the systems II and III resulting from a total of averaging steps of 5000–50,000 depending on the number of particles.

## 5.2 Systems

At present the only possibility to study theoretically cooperative phenomena at the vicinity of a critical point of fluids is offered by computer-simulations of

real systems. For that purpose we have chosen the simplest binary fluid mixtures which show a critical mixing point and whose molecules can approximately be regarded as spherically symmetric.

As far as a genuine liquid-liquid (L-L) phase separation is concerned, we were confined to the mixture  $\text{CH}_4/\text{CF}_4$ . Although the molecules of this system bear an octupole moment and have rotational degrees of freedom, it is reasonable to describe the interaction of these molecules in a first step by spherically symmetric potentials. Furthermore this binary liquid mixture is well investigated experimentally and hence the 1-2 pair-potential function has been evaluated from measurements of the second virial coefficient.<sup>50</sup> Additionally our own MDC on pure liquid methane based on (12-6) Lennard-Jones (L-J) potentials had led to satisfactory agreement with experiment.<sup>51</sup>

The system I,  $\text{CH}_4/\text{CF}_4$ , exhibits an upper critical mixing point at  $T_c = 94.5 \text{ K}$  and  $x_1 = 0.57$  under its saturation pressure. For the rest of this report, the subscript 1 shall always refer to the first component of a system A/B, and  $x$  shall denote the mole fraction if not explained otherwise. In Figure 1 we show the  $T, x$ -phase diagram of  $\text{CH}_4/\text{CF}_4$  under its saturation pressure measured by Scott *et al.*<sup>52</sup>

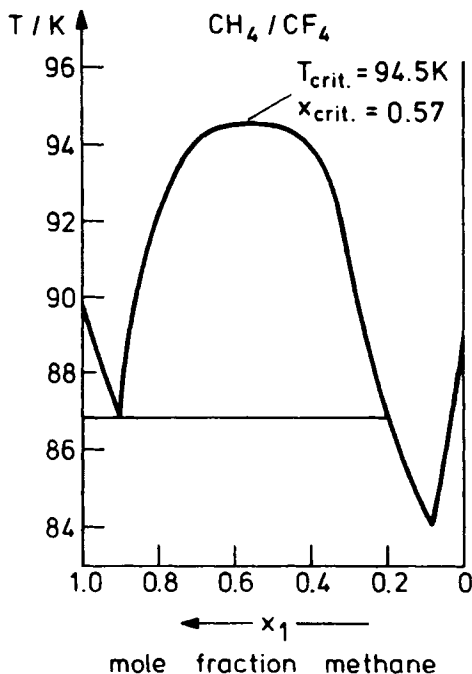


FIGURE 1  $T, x$ -projection of the phase diagram for system I at the saturation pressure.<sup>52</sup>

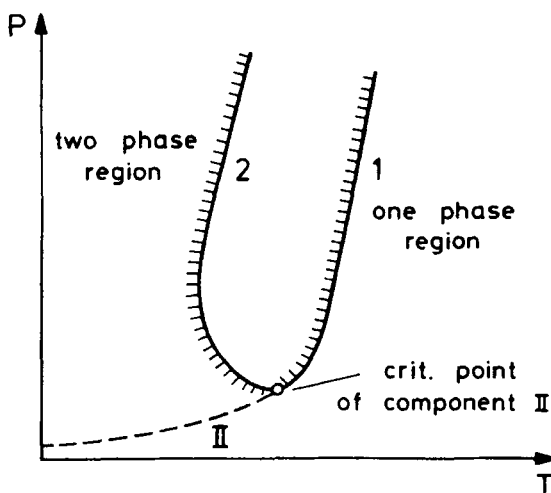


FIGURE 2  $P, T$ -projection of a phase diagram showing gas-gas equilibria of the first, 1, and the second type, 2, for a binary fluid.

We have carried out calculations for the complete concentration range and temperatures between 95 and 150 K for the homogeneous part of the phase region of the experimental system. The temperature interval lies below the critical temperatures of the pure substances and near the melting temperatures  $T_f$ :

$$\begin{aligned} T_c^{\text{CF}_4} &= 225 \text{ K}, & T_c^{\text{CH}_4} &= 192 \text{ K}; \\ T_f^{\text{CF}_4} &= 90 \text{ K}, & T_f^{\text{CH}_4} &= 91 \text{ K}. \end{aligned}$$

The densities of the pure substances were taken from the common literature, for the densities of the mixture we used average values which differed unremarkably from the values experimentally determined for a few temperatures.<sup>12,52</sup>

In contrast to system I, the systems II and III, Ne/Kr and He/Xe, are much better suited for MDC. These rare-gas mixtures show "gas-gas phase separation" found by Trappeniers *et al.*<sup>53</sup> and by De Swaan Arons *et al.*<sup>54</sup> The system III undergoes a gas-gas equilibrium of the first type, while system II shows an equilibrium of the second type. The structure of those equilibria is in detail discussed by Schneider.<sup>15</sup>

For a gas-gas equilibrium of the first type the critical line runs monotonously to higher pressures at higher temperatures, whereas for an equilibrium of the second kind a temperature minimum is passed. In Figure 2 we have schematically plotted a  $P, T$ -projection of a  $P, T, x$ -surface of a binary system showing gas-gas equilibria of the first, 1, and the second kind, 2.<sup>15</sup>

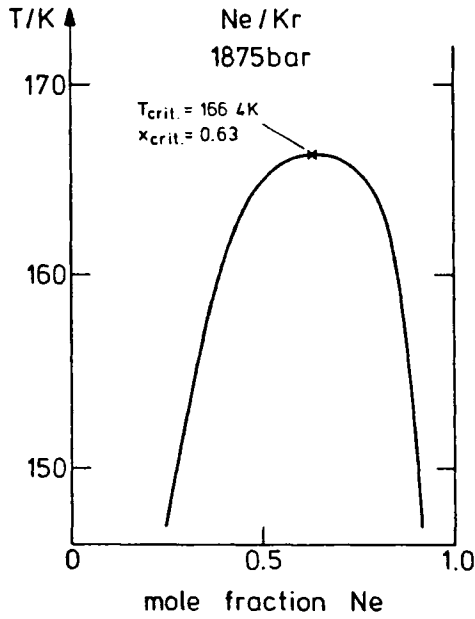


FIGURE 3  $T, x$ -projection of the phase diagram for system II.<sup>53</sup>

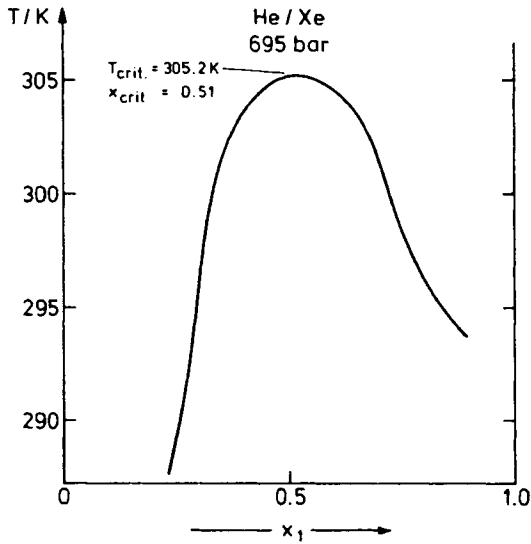


FIGURE 4  $T, x$ -projection of the phase diagram for system III.<sup>54</sup>

TABLE II

Densities calculated from the R-K equation of state

$\rho$ [g/cm <sup>3</sup> ]	Ne/Kr (1800 bar):	
	$T$ [K]	$x_1$ (Ne)
2.2246	230	0.2
2.3118	200	0.2
2.4018	170	0.2
1.8300	230	0.5
1.9182	200	0.5
2.0121	170	0.5
1.3449	230	0.8
1.4256	200	0.8
1.5152	170	0.8

The most reliable calculations, basical for all the present problems, have been performed for the system II, Ne/Kr.

In Figure 3 we show the phase-diagram of this system II, as it is measured by Trappeniers *et al.*<sup>53</sup> The upper critical mixing point lies at  $T_c = 166.4$  K,  $x_1 = 0.63$ , under a pressure of 1875 bar.

Simulations were done for temperatures of 150 K–250 K and for the whole concentration range. The densities were calculated from a Redlich–Kwong (R–K) equation of state which had been fitted to experimental PVT-data and phase-equilibrium data for the high-pressure range.<sup>55</sup>

In a similar way we obtained the density of system III. A few densities of the mixture Ne/Kr are presented on Table II.

For further comparisons we have performed MDC on system III. However, the calculations on this system are only of secondary importance with respect to the problems considered here, particularly, because system III is another example of a “gas–gas phase separation.”

For completeness, we have drawn the  $T, x$ -diagram of system III in Figure 4. The upper critical mixing point is located at  $T_c = 305.2$  K and  $x_1 = 0.51$  under a pressure of 695 bar.<sup>54,56</sup>

### 5.3 Molecular interaction potentials

The interaction potentials for the molecules contained in the three mixtures were approximated by L–J (12–6)-potential functions:

$$u(r) = 4\epsilon \left[ \left( \frac{\sigma}{r} \right)^{12} - \left( \frac{\sigma}{r} \right)^6 \right] \quad (6)$$

The two-parameter potential functions are regarded as appropriate effective pair-potentials for the simulation of real liquids and liquid mixtures by



MDC. Thus our calculations for the region of the critical point should be based on these potential functions, too.

It is partly possible to simulate a liquid in terms of a hard-core potential, because the repulsive part of the potential function plays the main part in systems of condensed molecules.<sup>57</sup> The modelling of cooperative effects, however, seems to require also the attractive term of the potential function.<sup>58, 59</sup> Additionally for L-J potential functions, there exists a great deal of experimental and theoretical experience for deriving the potential parameters from the second virial coefficient and viscosity numbers, specifically, when rare-gases are considered.

For system I the interactions 1-1, 2-2 and 1-2 have been experimentally evaluated in terms of relative volume and energy parameters by measurements of the second virial coefficient and of the viscosity coefficients.<sup>13, 50</sup>

Table III lists the  $\epsilon$ ,  $\sigma$  parameters used for the L-J potentials of system I. Both values,  $\epsilon_{12}$  and  $\sigma_{12}$ , differ appreciably from the values predicted by the Lorentz-Berthelot rules. The energy parameter is even smaller than  $\epsilon_1$  or  $\epsilon_2$ . This appears to be the usual case for fluorocarbon/hydrocarbon systems.<sup>13</sup> The Lorentz-Berthelot rules, however, do by no means predict valuable 1-2 potentials for most of the real mixtures, a much better description of the 1-2 interaction is however achieved by refined mixing rules proposed by Kohler.<sup>59</sup>

These "experimental" L-J parameters were applied to all our MDC on system I and the pure substances without further adjustment.<sup>12</sup> While the calculated SDC of the pure liquids, CH<sub>4</sub> and CF<sub>4</sub>, agreed well with the experimental values, as seen from Figure 5, the compressibility factors showed larger deviations from the experimental ones, especially the theoretical values for CF<sub>4</sub> exceeded the experimental numbers by more than one order of magnitude. It is now known that (12-6)-potential functions are insufficient for such globular molecules in the liquid state and have to be replaced by functions with a larger repulsive part, as (18-6) or (24-6)-potentials.<sup>49, 60</sup> Our later preliminary calculations based on (18-6)-potentials reproduced well the experimental compressibility factors and

TABLE III  
Lennard-Jones potential-parameters<sup>13</sup>

	CH <sub>4</sub> /CF <sub>4</sub> (system I)	
	$\epsilon/k_B^*$ [K]	$\sigma$ [Å]
CH <sub>4</sub>	139.0	3.822
CH <sub>4</sub> -CF <sub>4</sub>	127.5	4.327
CF <sub>4</sub>	141.4	4.747

\* Boltzmann constant.

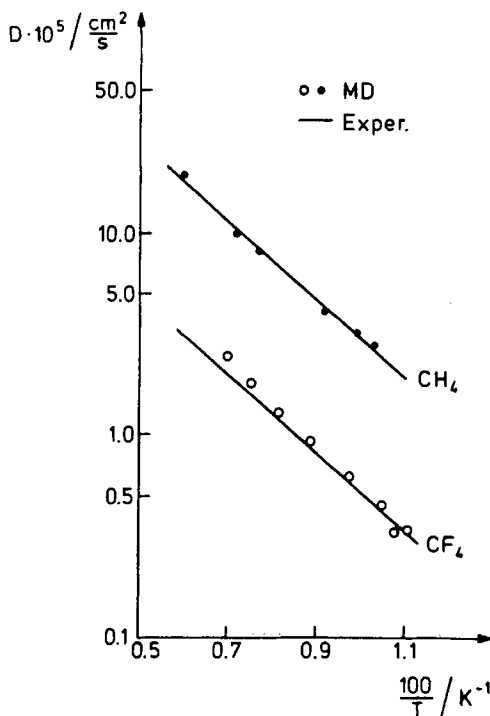


FIGURE 5 SDC of pure liquid CH<sub>4</sub> and CF<sub>4</sub> as function of temperature at the saturation pressure.<sup>12</sup>

additionally indicated that the results for the mixture at about equimolar concentration resembled those calculated on the (12-6)-potentials. Apparently the draw-back of the (12-6)-potential for the description of the CF<sub>4</sub>-interaction has little effect on MDC for the mixture around equimolar composition. Our results at higher CF<sub>4</sub>-concentrations will therefore not be interpreted.

For the systems II and III we have initially chosen the  $\epsilon$  and  $\sigma$ -parameters commonly proposed by the literature.<sup>61</sup> In subsequent steps the 1-1 and 2-2 parameters as well as the 1-2 parameters were corrected in the way described below. The parameters finally obtained are listed in Table IV. The two systems II and III, are certainly not to be regarded as "ideal" mixtures, at least not at this range of liquid-like densities under high pressure. While for system I the three interaction potentials have roughly equal potential-minima, the interactions for the latter are extremely different.

The mass ratio of the molecules is comparable for system I and II and amounts to  $\sim 4$ , but for system III this ratio reaches the value of  $m_{\text{Xe}}/m_{\text{He}} \sim 35$ . The fitting procedure for the  $\epsilon$ ,  $\sigma$ -values was first carried out on the pure substances. The values of the 1-1 and 2-2 interaction were changed to reproduce

TABLE IV  
Lennard-Jones potential-parameters<sup>62</sup>

Ne/Kr (system II)		
	$\varepsilon/k_B^a$ [K]	$\sigma$ [Å]
Ne	34.2	2.86
Ne-Kr	64.6	3.26
Kr	167.0	3.67
He/Xe (system III)		
	$\varepsilon/k_B^a$ [K]	$\sigma$ [Å]
He	10.8	2.570
He-Xe	44.6	3.7586
Xe	224.0	3.385

<sup>a</sup> Boltzmann constant.

by MDC the experimental transport coefficients and the compressibility factors (CF) of liquid Ne, Kr and Xe. Experimental SDC and CF only exist for the low pressure range, so that our computations were limited to this region. From Figure 6 we can see the agreement between the theoretical and experimental SDC of pure Ne and Kr.<sup>62</sup> The calculated CF also fitted well into the experimental ones providing a reliable simulation basis for the pure liquids.

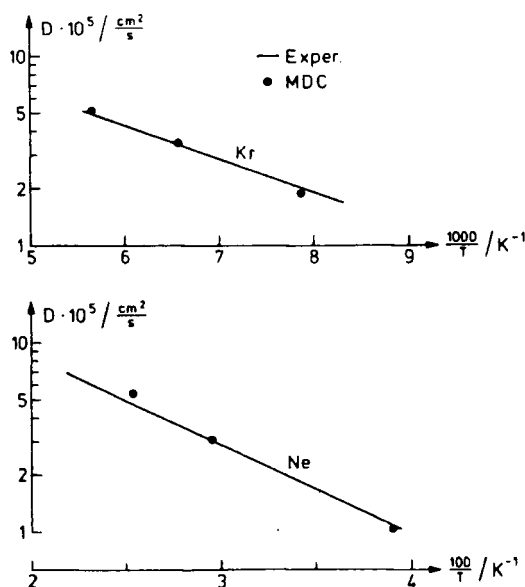


FIGURE 6 SDC of pure liquid Ne and Kr as function of temperature at low pressures.<sup>62</sup>

The subsequent MDC on the mixtures were to indicate the validity of these potentials for the simulation of the high-pressure range. As we have already mentioned, the existing PVT-data for the mixtures have been applied to an R-K equation of state.<sup>62</sup> According to common experience this R-K equation reproduces well the experimental values within a wide range. So the use of the R-K equation was two-fold: firstly, to compare directly the MDC-CF with the experimental ones, secondly, to adjust the  $\epsilon_{12}$ ,  $\sigma_{12}$  values by the a, b-parameters occurring in the R-K equation of state.<sup>55</sup> For the interaction of unlike pairs we obtained in this way a correction due to the non-ideality of the mixtures. These values for system II and III are listed on Table IV. It is seen from this table that for system II  $\epsilon_{12}$  is about 20% smaller than the "ideal" value  $\sqrt{\epsilon_1 \cdot \epsilon_2}$ , for system III more than 10%.  $\sigma_{12}$  is little changed for system II, but for system III about 15% relative to the "ideal" value,  $\sigma_{12} = \frac{1}{2}(\sigma_1 + \sigma_2)$ .<sup>63</sup>

With these 1-2 potentials and the use of the 1-1, 2-2 potentials initially adjusted, we were able to reproduce the experimental CF of the mixtures for the high-pressure range. Since the pressure is a quantity strongly dependent on the effective potentials inserted in MDC, we regarded this agreement as a definite indication of the application of these potentials to our MDC.<sup>64</sup> The results will in particular be discussed in the subsequent article.<sup>1</sup>

## References

1. C. Hoheisel, *Phys. Chem. Liquids*, 1979, subsequent paper.
2. H. Bertagnolli, D. O. Leicht, and M. D. Zeidler, *Molec. Phys.*, **35**, 139 (1978).
3. P. A. Egelstaff and J. W. Ring, *Physics of Simple Liquids*, (North-Holland), 1968.
4. J. M. H. Levelt Sengers, "High Pressure Technology," Vol. II (Marcel Dekker), 1977.
5. K. Binder, *Phase Transitions and Critical Phenomena*, Vol. 5b, edited by C. Domb and M. S. Green (Academic Press), 1976.
6. F. H. Ree, *Physical Chemistry: An Advanced Treatise*, VIII A, edited by H. Eyring, D. Henderson, and W. Jost (Academic Press), 1971.
7. D. J. Adams, *Molec. Phys.*, **37**, 211 (1979).
8. J. P. Hansen and L. Verlet, *Phys. Rev.*, **184**, 151 (1969).
9. H. J. Raveche, R. D. Mountain, and W. B. Streett, *J. Chem. Physics*, **62**, 4582 (1975).
10. J. V. Sengers and J. M. H. Levelt Sengers, *Progress in Liquid Physics*, edited by C. A. Croxton (Wiley Interscience), 1978.
11. W. W. Wood, *Physics of Simple Liquids* (North-Holland), 1968.
12. C. Hoheisel, *Ber. Bunsenges. Phys. Chem.*, **81**, 462 (1977).
13. J. R. Rowlinson, *Liquids and Liquid Mixtures*, 2nd Edition (Butterworths), 1969.
14. R. Haase, *Thermodynamik der Mischphasen* (Springer Verlag), 1956.
15. G. M. Schneider, *Advances in Chemical Physics*, Vol. XVII, edited by I. Prigogine and S. A. Rice (Wiley Interscience), 1970.
16. R. Haase, *Thermodynamik irreversibler Prozesse* (D. Steinkopff), 1963.
17. R. Haase and M. Siry, *Z. Phys. Chem.*, NF **57**, 56 (1968).
18. I. R. Krichewskij and Tsekhanskaya, *Zhur. Fiz. Khim.*, **30**, 2315 (1956).
19. J. Thoen, E. Bloemen, and W. Van Dae, *J. Chem. Phys.*, **68**, 735 (1978).
20. G. D'Arrigo, L. Mistura, and P. Tartaglia, *J. Chem. Phys.*, **66**, 80 (1977).
21. M. Fixmann, *J. Chem. Phys.*, **36**, 310 (1962).

22. P. Kruus and T. A. Bak, *Acta Chem. Scand.*, **20**, 231 (1966).
23. H. Hamann, C. Hoheisel, and H. Richterling, *Ber. Bunsenges. Phys. Chem.*, **76**, 249 (1972).
24. S. H. Chen, *Physical Chemistry: An Advanced Treatise*, VIII A, edited by H. Eyring, D. Henderson, and W. Jost (Academic Press), 1971.
25. A. Münster and K. Sagel, *Bunsenges. Phys. Chem.*, **62**, 1075 (1958).
26. R. Fürth and C. L. Williams, *Proc. Roy. Soc.*, **A224**, 104 (London), 1954.
27. C. Hoheisel, *Diplomarbeit Göttingen*, (1967).
28. A. G. Chynoweth and W. G. Schneider, *J. Chem. Phys.*, **19**, 1566 (1951).
29. F. Kohler and O. K. Rice, *J. Chem. Phys.*, **26**, 1614 (1957).
30. G. W. Brady, *J. Chem. Phys.*, **32**, 45 (1960).
31. B. Volochine, *Ber. Bunsenges. Phys. Chem.*, **76**, 217 (1972).
32. G. W. Brady and J. I. Petz, *J. Chem. Phys.*, **34**, 332 (1961).
33. L. Van Hove, *Phys. Rev.*, **93**, 268 (1954).
34. R. A. Howe, *Progress in Liquid Physics*, edited by C. A. Croxton (Wiley Interscience), 1978.
35. H. E. Stanley, G. Paul, and S. Milosevic, *Physical Chemistry: An Advanced Treatise*, VIII B, edited by H. Eyring, D. Henderson, W. Jost (Academic Press), 1971.
36. J. S. Rowlinson and M. Evans, *Annu. Rep. Chem., Sect. A, Phys. Inorg. Chem.*, 5-30 (1975).
37. M. E. Fisher, *Rep. Prog. Phys.*, **30**, 615 (1967).
38. K. Kawasaki, *Phase Transitions and Critical Phenomena*, Vol. 5 B, edited by C. Domb, M. S. Green (Academic Press), 1975.
39. F. Zernike, *Proc. Acad. Sci.*, **18**, 1520 (Amsterdam), 1916.
40. J. Stephenson, *Physical Chemistry: An Advanced Treatise*, VIII B, edited by H. Eyring, D. Henderson, and W. Jost (Academic Press), 1971.
41. B. Chu, *Ber. Bunsenges. Phys. Chem.*, **76**, 202 (1972).
42. G. Arcovito, C. Faloci, M. Roberti, and L. Mistura, *Phys. Rev. Lett.*, **22**, 1040 (1969).
43. A. V. Voronel, *Phase Transitions and Critical Phenomena*, Vol. 5b, edited by C. Domb, and M. S. Green (Academic Press), 1976.
44. P. C. Hohenberg and B. I. Halperin, *Rev. Mod. Phys.*, **49**, 435 (1977).
45. B. J. Berne, *Physical Chemistry: An Advanced Treatise*, Vol. VIII B, edited by H. Eyring, D. Henderson, and W. Jost (Academic Press), 1971.
46. P. G. Watson, *Phase Transitions and Critical Phenomena*, Vol. 2, edited by C. Domb and M. S. Green (Academic Press), 1973.
47. A. Rahmann, *Phys. Rev.*, **136A**, 405 (1964).
48. F. Vesely, *Computereperimente an Flüssigkeitsmodellen* (Physik Verlag), 1978.
49. C. Hoheisel and U. Deiters, *Ber. Bunsenges. Phys. Chem.*, **81**, 1225 (1977).
50. D. R. Douslin, R. H. Harrison, and R. T. Moore, *J. Phys. Chem.*, **71**, 3477 (1967).
51. C. Hoheisel, *Ber. Bunsenges. Phys. Chem.*, **80**, 985 (1976).
52. M. I. Croll and R. L. Scott, *J. Phys. Chem.*, **62**, 954 (1958).
53. N. J. Trappeniers and J. A. Schouten *Physica*, **33**, 379 (1974).
54. J. De Swaan Arons and G. A. M. Diepen, *J. Chem. Phys.*, **44**, 2322 (1966).
55. U. Deiters and G. M. Schneider, *Ber. Bunsenges. Phys. Chem.*, **80**, 1316 (1976).
56. P. Zandbergen, H. F. P. Knapp, and J. J. M. Beenakker, *Physica*, **33**, 379 (1967).
57. F. Kohler, *Ber. Bunsenges. Phys. Chem.*, **81**, 1037 (1977).
58. B. J. Alder, D. A. Young, and M. A. Mark, *J. Chem. Phys.*, **56**, 3016 (1972).
59. H. N. V. Temperley, *Progress in Liquid Physics*, edited by C. A. Croxton (Wiley Interscience), 1978.
60. C. Hoheisel and M. D. Zeidler, *Ber. Bunsenges. Phys. Chem.*, **83**, 28 (1979).
61. J. O. Hirschfelder, C. F. Curtis, and R. B. Bird, *Molecular Theory of Gases and Liquids* (Wiley Interscience), 1967.
62. C. Hoheisel and U. Deiters, *Molec. Phys.*, **37**, 95.
63. U. Deiters, *Thesis Bochum*, (1979).
64. J. A. Barker and D. Henderson, *Rev. Mod. Phys.*, **48**, 587 (1976).